PROGRESS IN PHOTOVOLTAICS: RESEARCH AND APPLICATIONS
Prog. Photovolt: Res. Appl. 2011; **19**:977–982
Published online 23 July 2010 in Wiley Online Library (wileyonlinelibrary.com). DOI: 10.1002/pip.1013

RESEARCH: SHORT COMMUNICATION

Degradation of individual cells in a module measured with differential *IV* analysis

G.B. Alers[1]*, J. Zhou[2], C. Deline[3], P. Hacke[3] and S.R. Kurtz[3]

[1] Department of Physics, University of California, Santa Cruz, CA 95066, USA
[2] Department of Electrical Engineering, University of California, Santa Cruz, CA 95066, USA
[3] National Renewable Energy Laboratory, Golden, CO, USA

ABSTRACT

A methodology is developed for the extraction of cell-level properties from the analysis of differential *IV* response in a solar module with series connected cells. Through a combination of simulation and experimental verification we show that the shunt resistance and short circuit current of individual cells can be determined from a peak in the module differential resistance with cells that are partially shaded. The magnitude of the peak is equal to the shunt resistance of the cell for small values of shunt resistance. The current at which the peak occurs is proportional to the product of the short circuit current and the shading factor of the particular cell. With this methodology, we are able to measure degradation of 72 individual cells in a single commercial module after a high temperature/high humidity/high voltage stress test. Therefore, the statistics of degradation in this test were improved 72-fold. Copyright © 2010 John Wiley & Sons, Ltd.

KEYWORDS

solar; module; reliability; differential resistance; shunt resistance; series resistance

***Correspondence**

G.B. Alers, Department of Physics, University of California, Santa Cruz, CA 95066, USA.
E-mail: galers@ucsc.edu

Received 3 January 2010; Revised 13 May 2010

1. INTRODUCTION

Qualification testing procedures for photovoltaic modules can be very time consuming and costly. The number of modules used in a stress test is usually small, on the order or 2–4 modules due in part to the cost and physical size of the photovoltaic modules. After the tests are completed, a single module either passes or fails the test—resulting in only one data point per module. The lack of statistics makes it difficult to collect quantitative information on degradation rates. The ability to make lifetime projections usually relies on an abundance of data so that a statistical approach can be applied for the probability of failure after a given time.

Degradation in performance of a photovoltaic module will include the additive degradation of multiple cells in the module. Typically, 50–100 individual cells are attached in series in a module to increase the voltage output. Each of these cells may degrade differently depending on pre-existing defects or the physical location in the module (in the case of corrosion) [1]. If one is able to measure the degradation of an individual cell in a module after a qualification test or outdoor testing then the statistics of degradation could be improved 50–100-fold. However, extracting performance parameters of individual cells in a packaged module is complicated because contact to individual cells cannot be achieved without de-packaging the module [2].

Several methods have been proposed to extract individual cell properties from module level data. Some methods involve completely shading a cell to measure the dark-*IV* curve in forward or reverse bias [3]. However, achieving 100% shading in a fully packaged module can be difficult due to the transmission of light through the top glass layer from internal reflection. Other methods have been suggested using lock-in techniques [4] to measure effective impedance of the shaded cell, a scanning laser [5] or lock-in thermography [6]. However, these methods require specialized equipment. As an alternative, we consider calculating the differential impedance [7] directly from DC *IV* curves taken with a conventional curve tracer.

In this paper, we describe a method to extract the shunt resistance (R_{sh}) and output current of individual cells through partial shading of cells in a module under full illumination. The test is similar to standard hot spot tests in

which the cell that runs hottest when shaded (often the lowest shunt resistance) is chosen for stressing [8,9], but this test has a different purpose and is more quantitative especially for very low shunt resistances that are typical for degraded modules. Standard *I–V* curves for the module with a shaded cell are used to obtain the cell shunt resistance R_{sh} [10,11] at nominally zero bias conditions using the maximum in differential impedance dV/dI and d^2V/dI^2. Partial shading is used instead of full shading to measure the output current of the cell as determined by the current at which the peak in differential resistance occurs. Partial shading also eliminates the need to remove bypass diodes that might be present. Results from simulation show very good agreement between R_{sh} measured with this method and R_{sh} chosen for the model. Shunt resistances are extracted in reverse bias, so no distinction can be made between a resistive shunt and weak diode. The technique is most accurate for low shunt resistance values of a cell. At high R_{sh} values, the nonlinear nature of the reverse biased cell near breakdown can lead to deviations between the values extracted from the differential impedance and those within the model. However, degraded cells usually exhibit small shunt resistances making this the primary region of interest [12].

2. SIMULATION RESULTS

The photovoltaic simulation packaged PVSIM developed by D. L. King, J. K Dudley and W. E. Boyson at Sandia National Laboratories [13] was used to model the *IV* curves for a 72 cell single crystalline silicon module. The simulation uses the standard two-diode model for the module *IV* curve [10] and was able to calculate the impact of partial shading on current–voltage behavior of a module by setting the output current of one cell to 50% of its nominal value. The cell parameters used for the simulation are listed in Table I and are based on typical values measured for commercial modules [14]. The diode ideality factor of 3.7 was determined empirically from fitting the *IV* curves of these modules and does not have physical significance. The simulated *IV* curve for a module with one 50% shaded cell at a range of R_{sh} values is shown in Figure 1. The *IV* curve for the unshaded module, also plotted in Figure 1, is monotonic with a low effective impedance at V_{oc} and high effective impedance at I_{sc}. In the shaded modules there is a well-defined ''kink'' in the *IV* curve that corresponds to the current at which the shaded cell limits the output current and becomes reverse biased. The ''kink'' in the *IV* curves is present because at 50% illumination relative to the other cells in the module, the current output of the shaded cell is effectively limited to 50% of the unshaded cell current. When the photocurrent of the other cells in the module exceeds the output current of the shaded cell then this cell becomes the current limiting element in the chain and a reverse bias voltage is generated across the shaded cell. Assuming precisely 50% shading, the current–voltage behavior of the module at currents larger than 50% of I_{sc} is determined by the reverse characteristic of the shaded cell's *IV* curve. At higher currents, bypass diodes, if present, shunt the voltage across the string that includes the shaded cell.

Table I. Default cell parameters used for the simulation of the *IV* curves for a 72 cell module with 100 mm cells connected in series in three strings and including three bypass diodes.

Default cell data for simulations	
I_{sc}	3 A
R-series	0.01 Ω
R-shunt	40 Ω
ln(ideal diode recombination)	−21 A
ln(non-ideal recombination)	−8 A
Non-ideal diode quality factor	3.7
Breakdown voltage	−8 V
Fraction of shunt current in breakdown	0.5
Avalanche breakdown exponent	1
Temperature	25 °C
Illumination	1000 W/m^2

Figure 2 shows the simulated differential impedance, dV/dI in the region of the ''kink'' which has a local maximum in effective resistance. The differential resistance dV/dI at this local maximum corresponds closely to dV/dI for the unshaded module at the same current, summed with the R_{sh} of the shaded cell. The magnitude of this local dV/dI peak is calculated for multiple simulated R_{sh} values of the 50% shaded cell. Additionally, two values of reverse breakdown voltage threshold are simulated −8 V and −24 V. These results are presented in Figure 3.

There are several contributions to the current in a cell under reverse bias such as the cell shunt resistance, generation–recombination current and junction breakdown current. The shunt resistance R_{sh}, by definition, is ohmic

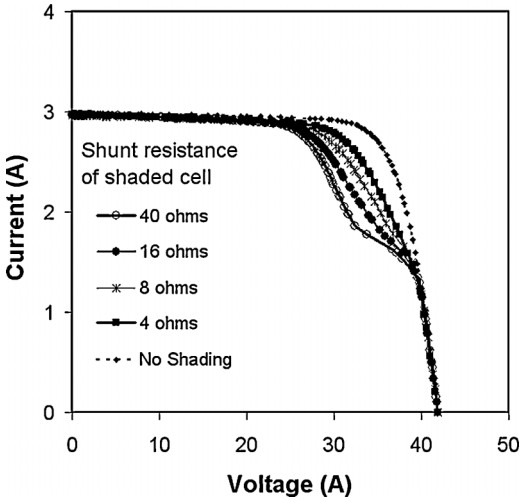

Figure 1. Simulation results for the module specified in Table I with one cell shaded 50% and a range of shunt resistances for that cell.

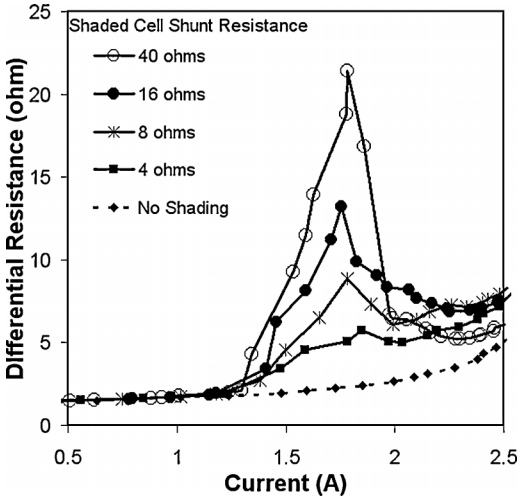

Figure 2. Simulation results for the differential resistance d*V*/d*I* in the region of the ''kink'' in the *IV* response. A peak in the differential resistance is observed that correlates well with the shunt resistance of the shaded cell.

with a current that is proportional to voltage. The reverse avalanche breakdown current on the other hand is nonlinear. The two terms together describe the reverse leakage current I_{shunt} [14]:

$$I_{\text{shunt}} = \frac{V}{R_{\text{sh}}}\left\{1 + a\left(1 - \frac{V}{V_{\text{br}}}\right)\right\}^{-m} \qquad (1)$$

where, V is the voltage across the cell junction, a is the fraction of shunt current involved in reverse breakdown (assumed to be 0.5), V_{br} is the junction breakdown voltage (assumed to be -8 V) and m is the avalanche breakdown exponent determined empirically to be 3.7. Values used in the simulations for these parameters are given in Table I.

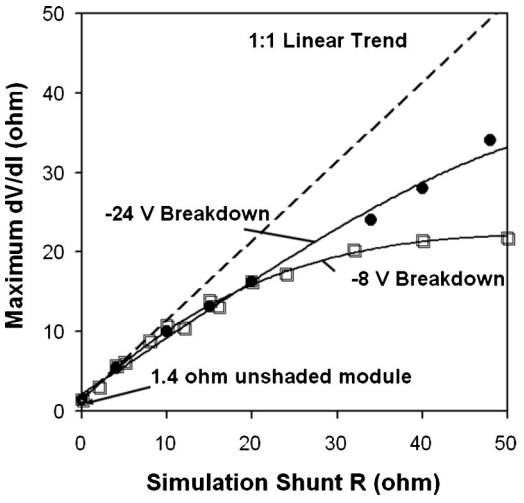

Figure 3. Simulation results for local maximum in d*V*/d*I* for a shaded cell of varying R_{sh}. Two values for reverse breakdown voltage are simulated: -8 V (open square) and -24 V (filled circle). The lines through the data are guides.

Reverse breakdown currents will effectively add to the current of the ohmic shunt, resulting in a larger differential conductance (d*I*/d*V*) and conversely a smaller differential resistance (d*V*/d*I*). Therefore, the maximum in d*V*/d*I* will occur when voltage across the cell V is near zero and only the first term of the sum in Eq. (1), or the ohmic portion of the cell impedance contributes to the differential impedance. Other contributions to current will decrease d*V*/d*I* at larger reverse bias so d*V*/d*I* will no longer be a valid indicator of the cell's value of R_{sh}. Therefore, a peak in measured d*V*/d*I* is consistent with a minimum in reverse bias leakage current, and this value of d*V*/d*I* is expected to be close to the cell's value of R_{shunt}. This relationship holds true if R_{sh} is small and other leakage mechanisms are effectively shorted by the shunt resistance. Figure 3 shows good agreement in the simulation between the local maximum of d*V*/d*I* and R_{sh} for low shunt resistances ($<12\ \Omega$/cell). At higher values of R_{sh} and smaller values of breakdown threshold V_{br} the breakdown current makes a larger contribution and d*V*/d*I* is effectively lowered below the simulated value of R_{sh}.

In the limit of zero shunt resistance (a completely shorted cell), d*V*/d*I* for a module will not change when a cell is shaded, making it impossible to extract any additional information. If R_{sh} is very small ($<1\ \Omega$ /cell) then it can be difficult to separate the differential impedance of the shaded cell from the differential impedance of the module. In this case, it might be necessary to use the second derivative of the current–voltage curves to identify the maximum change in d*V*/d*I*. The addition of a small shunt resistance from a shaded cell to the module's differential resistance would appear as a step in d*V*/d*I* and not a peak. A step in d*V*/d*I* would result in a peak in dV^2/dI^2. However, *IV* curves need to be collected very accurately to identify a peak in d^2V/dI^2 above the noise in the measurement.

The voltage at which d*V*/d*I* reaches a maximum is proportional to the short circuit current, I_{sc}, of the partially shaded cell. The current at which this peak in differential impedance occurs is at $F_{\text{s}} \times I_{\text{sc}}$, where F_{s} is the fraction of shading for the cell. The exact current at which this occurs, I_{peak}, depends on the exact amount of shading and the effective output impedance of the other cells in the module that are forcing the current. Therefore, this partial-shading test also provides information on the short circuit current of the shaded cell.

3. APPLICATION

This cell-level R_{sh} and I_{sc} measurement technique was applied to two polycrystalline silicon modules, each composed of 72–150 mm^2 cells in series with bypass diodes in parallel with three 24-cell strings [15,16]. One module was new and had not undergone stress testing. A second functionally identical module underwent stress

testing for 1000 h at 85 °C, 80% relative humidity and 600 V applied between the cells and the frame of the module. Figure 4 shows the R_{sh} distribution across the module for the unstressed module (a) and the stressed module (b). The range of R_{sh} measured for the unstressed module was 60–600 mΩ/cm^2 (9–100 Ω/cell) after subtracting dV/dI at $I_{peak} = 7.7$ mΩ/cm^2 (1.2 Ω/cell) measured in the unshaded reference condition. The R_{sh} distribution in the unstressed module followed a log-normal distribution with a width of $\sigma = 1.0$ as shown in Figure 4. A normal (Gaussian) distribution of ln(R_{sh}) appears as a straight line when plotted in this way. For the stress tested module, the distribution in R_{sh} is much broader with a width of $\sigma = 1.4$ and a distribution between 3 and 400 mΩ/cm^2 (0.5–62 Ω/cell). A constant dV/dI = 17 mΩ/cm^2 (2.6 Ω/cell) was subtracted from the R_{sh} measurement to account for the reference unshaded condition at I_{peak}, compared with the unstressed module, the peak output power of the stressed module dropped from 160 to 64 W, open circuit voltage dropped from 43.5 to 39.5 V and short circuit current dropped from 5.0 to 4.8 A. This degree of degradation is considered a failure for the test that these modules were a part of. Analysis of R_{sh} for each cell after the test permits greater quantification of the degradation of the module. Figure 5 shows the spatial pattern of the shunt resistance measured with this technique and Figure 4 shows the log-normal distribution of shunt resistances. The spatial pattern of degradation shows a greater concentration of failed cells near the right-hand edge of the module shown in Figure 5. This is consistent with a visual inspection of the module that showed greater corrosion and discoloration of the cells at this edge. By measuring R_{sh} for each cell, degradation at this edge of the module can be better quantified. The damp heat test + high voltage appears to degrade cells near the frame where the electric field is the highest for the applied voltage. This degradation can be quantified by a decrease in shunt resistance.

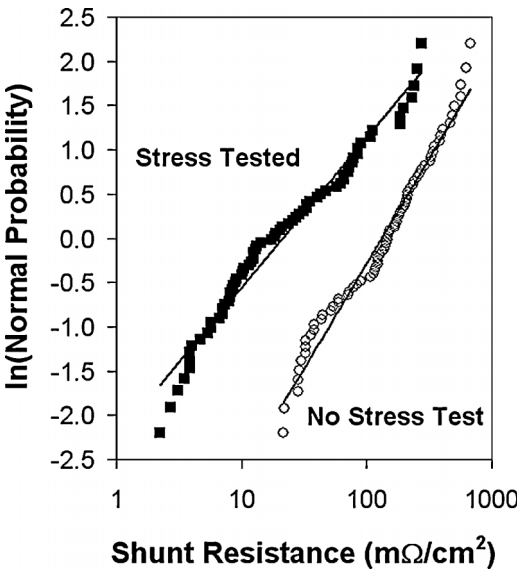

Figure 4. Log-normal distribution of the shunt resistance in an unstressed module (open circles) and a stressed module (filled squares). The distribution of shunt resistances broadens and moves towards a smaller value after stressing.

88	9	26	31	3	5
92	278	198	109	6	6
79	189	114	73	6	5
64	242	50	167	6	8
60	23	24	8	8	10
47	9	10	28	11	16
13	189	233	9	10	11
21	68	15	35	10	15
16	38	12	45	29	15
12	81	74	87	36	11
21	11	68	20	15	14
7	256	7	7	33	7

Figure 5. Spatial pattern in the module of shunt resistance after stress testing. Dark gray colored cells have shunt resistance of 10 mΩ/cm^2 or less and light gray cells have shunt resistance between 10 mΩ/cm^2 and 15 mΩ/cm^2. Cells located near the module frame tend to show more failures.

For a given cell, measurement of I_{peak}, or the current corresponding to maximum dV/dI, provides an indication of that cell's I_{sc}. Neutral density filters used in this test were calibrated with a radiometer under full outdoor illumination. Some uncertainty will arise in the shading fraction from the placement of the neutral density filter on the module. This test is performed under full illumination to maximize current output and increase the sensitivity for very small values of shunt resistance observed in degraded modules. Current and voltage values need to be measured accurately to prevent excessive noise in the calculation of dV/dI and d^2V/dI^2. I_{peak} values for the cells of both

Prog. Photovolt: Res. Appl. 2011; **19**:977–982 © 2010 John Wiley & Sons, Ltd.
DOI: 10.1002/pip

modules are shown in Figure 6 as a percentage of that module's unshaded I_{sc}. For the unstressed module, the cells' I_{peak} values have an average of 0.54 times the module I_{sc} consistent with a shading fraction of 50%. The unstressed cell's I_{peak} measurement appears to be independent of its R_{sh} measurement. Variations in the measured value of I_{peak} can occur from variations in the exact placement of the filter on the module and slightly different output currents for the string that includes the shaded cell. For the stressed module, the distribution in I_{peak} is very broad for cells with low R_{sh} with I_{peak} values up to 20% lower than average. This correlation between R_{sh} and I_{peak} indicates that the maximum current of these cells has also been compromised by the stress test. The correlation does not apply to all cells, however, since some cells with R_{sh} less than 3 Ω still have an I_{peak} close to the average.

Several degradation mechanisms can lead to a decrease in shunt resistance of the cells. Localized ohmic shorts can form between the contacts of a single cell leading to a local shunt. Degradation of the photovoltaic material or the anti-reflection layer can lead to an increase in recombination currents and ultimately a low shunt resistance. Cracking or localized heating of the cell can form localized shorts. Once a cell is identified to have a low shunt resistance, imaging techniques such as infrared or electroluminescence can be applied to better identify the mechanism. Here we have demonstrated that the degradation of individual cells can be monitored by measuring R_{sh} and I_{peak} of each cell. Performing these measurements before and after a stress test or during a test will allow quantification of the degradation rate of individual cells and increase the statistics for quantifying failure rates.

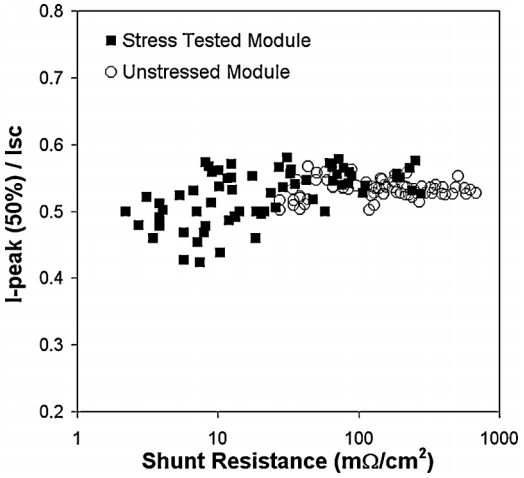

Figure 6. Correlation of measured shunt resistance and I_{peak}—the current that corresponds to a maximum in d*V*/d*I*. Cells with small shunt resistance tend to have a broader distribution and lower average output current.

4. CONCLUSION

A simple method is described for extracting the shunt resistance and I_{sc} of individual cells from the *IV* curves of a module with partial shading of cells. Modeling of the module level *IV* curves shows that the peak in d*V*/d*I* near $F_s \times I_{sc}$ is equivalent to the sum of R_{sh} for the cell and d*V*/d*I* for the unshaded module. The current at which d*V*/d*I* peaks is proportional to the short circuit current of the shaded cell. Therefore, the shunt resistance and short circuit current of individual cells can be obtained from a collection of *IV* curves for a module with individual cells partially shaded.

This methodology was applied to one unstressed module and a second module that had undergone stress testing for 1000 h at 85 °C and 85% relative humidity with 600 V applied between the module's active circuit and the module's frame. We show that prior to stressing, the shunt resistance of the individual cells has a log-normal distribution. After stress, the distribution in shunt resistances for the individual cells becomes broader with a significant fraction of the cells shunted with R_{sh} less than 3 Ω. Some of these cells also exhibit exceptionally low values of short circuit current. The cells with low shunt resistance are spatially located near the upper right corner of the module where visual evidence of electrochemically induced degradation was observed.

By measuring the shunt resistance and I_{sc} of individual cells, the degradation of individual cells can be extracted, greatly improving the statistics of the failure. The improved statistics can be used to monitor degradation rates of 72 (or more) individual cells from testing a single module.

ACKNOWLEDGEMENTS

This work was supported in part by the US Department of Energy grant number DE-FC36-08GO18014.A000.

REFERENCES

1. McMahon TJ. Accelerated testing and failure of thin-film PV modules. *Progress in Photovoltaics: Research and Applications* 2004; **12**: 235–248.
2. Alonso-Garcıa MC, Ruiz JM, Chenlo F. Experimental study of mismatch and shading effects in the *I–V* characteristics of a photovoltaic module. *Solar Energy Materials & Solar Cells* 2006; **90**: 329–340.
3. De Bernardez L, Buitrago RH. Dark *I–V* curve measurements of single cells in a photovoltaic module. *Progress in Photovoltaics: Research and Applications* 2006; **14**: 321–327.
4. McMahon TJ, Basso TS, Rummel SR. Cell shunt resistance and photovoltaic module performance, *Proceedings of the 25th IEEE Photovoltaic Specialists Conference, Washington DC*, 1996; 1291–1294.
5. Eisgruber IL, Sites JR. Extraction of individual-cell photocurrents and shunt resistances in encapsulated

modules using large-scale laser scanning. *Progress in Photovoltaics: Research and Applications* 1998; **4**: 63–75.
6. Thongpron J, Kirtikar K, Jivacate C. A method for the determination of dynamic resistance of photovoltaic modules under illumination. *Solar Energy Materials & Solar Cells* 2006; **90**: 3078–3084.
7. Thongpron J, Kirtikar K, Jivacate C. A method for the determination of dynamic resistance of photovoltaic modules under illumination. *Solar Energy Materials & Solar Cells* 2006; **90**: 3078–3084.
8. Wohlgemuth J, Herrmann W. Hot spot tests for crystalline silicon modules. *Proceedings of the 31st IEEE Photovoltaic Specialist Conference* 2005; 1062–1063.
9. Meyer EL, Ernest van Dyk E. The effect of reduced shunt resistance and shading on photovoltaic module performance., *Proceedings of the 31st IEEE Photovoltaic Specialist Conference* 2005; 1331–1334.
10. Chegaar M, Azzouzi G, Mialhe P. Simple parameter extraction method for illuminated solar cells. *Solid-State Electronics* 2006; **50**: 1234–1237.
11. Karatepe E, Boztepe M, Colak M. Development of a suitable model for characterizing photovoltaic arrays with shaded solar cells. *Solar Energy* 2007; **81**: 977–992.
12. Meyer EL, van Dyk EE. Characterization of degradation in thin-film photovoltaic module performance parameters. *Renewable Energy* 2003; **28**: 1455–1469.
13. King DL, Dudly JK, Boyson WE. PVSIM: a simulation program for cells, modules and arrays. *25th IEEE PVSC*, 1996; 1295–1297.
14. Bishop J. Computer simulation of the effects of electrical mismatches in photovoltaic cell interconnected circuits. *Solar Cells* 1988; **25**: 73–89.
15. Hacke P, Osterwald C, Trudell D, Terwilliger K, Bosco N, Gelak E, Kurtz S. Proceedings of the 19th Crystalline Silicon Workshop (Vail, CO, 2009).
16. Some of the parameters used in the simulations such as the non-ideal diode quality factor are empirical fitting parameters and do not have specific physical significance.